

The Effect of Photoconductive Mole Fraction Based on Thin Film $\text{Ba}_x\text{Sr}_{1-x}\text{TiO}_3$ ($x = 0.000; 0.125; 0.250; 0.375; 0.500$) on Electrical Properties and Diffusivity Coefficient

Irzaman^{1,*}, Vania Rahmawaty¹, Endah Kinarya Palupi¹, Nazopatul Patonah¹, Tony Sumaryada¹, Ridwan Siskandar², Husin Alatas¹, Muhammad Iqbal³, Brian Yuliarto³, Mohammad Zakki Fahmi⁴, Febdian Rusydi⁵, Widagdo Sri Nugroho⁶

¹ Department of Physics, Faculty of Mathematics and Science, Bogor Agricultural University, Meranti Street, Dramaga, Bogor, West Java, 16680, Indonesia

² Computer Engineering Study Program, College of Vocational Studies, IPB University, Bogor, West Java 16151, Indonesia; ridwansiskandar@apps.ipb.ac.id (R.S.);

³ Department of Engineering Physics, Industrial Engineering Faculty, Bandung Institute of Technology, Bandung, West Java 40132, Indonesia; iqbal@tf.itb.ac.id (M.I.); brian@tf.itb.ac.id (B.Y.);

⁴ Department of Chemistry, Faculty of Science and Technology, Airlangga University Surabaya, East Java 60115, Indonesia; m.zakki.fahmi@fst.unair.ac.id (M.Z.F.);

⁵ Department of Physics, Faculty of Science and Technology, Airlangga University Surabaya, East Java 60115, Indonesia

⁶ Department of Veterinary Public Health, Faculty of Veterinary Medicine, Universitas Gadjah Mada, Yogyakarta, Indonesia; weesnugroho@ugm.ac.id (W.S.N.);

* Correspondence: irzaman@apps.ipb.ac.id;

Scopus Author ID 7409571162

Received: 26.02.2021; Revised: 25.03.2021; Accepted: 28.03.2021; Published: 7.04.2021

Abstract: Barium Strontium Titanate ($\text{Ba}_x\text{Sr}_{1-x}\text{TiO}_3$) thin films have been fabricated for mole fraction ($x = 0.000; 0.125; 0.250; 0.375; 0.500$) on p-type silicon (100) substrate using Chemical Solution Deposition (CSD) method and spin coating technique. The film annealed at 850°C for 8 hours with an increasing rate of $1.67^\circ\text{C}/\text{minute}$. The BST thin film was characterized using an LCR meter that the film is given a different light intensity (0 lux, 4000 lux, 8000 lux). Data obtained from the LCR meter is conductance, capacitance, and impedance. Different mole fractions on Barium produce different electrical properties that show the value of electric conductivity, dielectric constant, impedance, and diffusion coefficient.

Keywords: $\text{Ba}_x\text{Sr}_{1-x}\text{TiO}_3$; mole fraction; electrical properties; diffusivity coefficient; LCR meter.

© 2021 by the authors. This article is an open-access article distributed under the terms and conditions of the Creative Commons Attribution (CC BY) license (<https://creativecommons.org/licenses/by/4.0/>).

1. Introduction

In recent years, increasing attention has been paid to the synthesis and characterization of barium strontium titanate (BST) because its uniqueness lies in its mole fraction, which can be varied and cause new chemical and physical properties. Partial substitution of Ba ions in pure $\text{Ba}_x\text{Sr}_{1-x}\text{TiO}_3$ strongly affects the ferroelectric-paraelectric phase transition temperature [1]. BST as a ferroelectric material has various technical advantages such as chemical stability, high permittivity, high dielectric constant, good thermal stability, and high tunability [2–7].

BST thin film is found in the perovskite family with general formula ABO_3 , which is the compositional modification in solid solution, substitution, and/or dopants. The addition of Ba atoms to the SrTiO_3 lattice substitutes the Sr atoms, influencing the crystalline structure and its properties⁶. Variation of BST mole fraction made is SrTiO_3 , $\text{Ba}_{0.125}\text{Sr}_{0.875}\text{TiO}_3$; $\text{Ba}_{0.25}\text{Sr}_{0.75}\text{TiO}_3$; $\text{Ba}_{0.375}\text{Sr}_{0.625}\text{TiO}_3$; and $\text{Ba}_{0.5}\text{Sr}_{0.5}\text{TiO}_3$. Many techniques can be applied to

prepare BST thin film, one of that is chemical solution deposition [3,8–16]. BST data retrieval is done using an LCRmeter to get the impedance, capacitance, and conductance data of BST measured with 3 variations, in dark conditions (0 lux) and light conditions (4000 lux and 8000 lux).

2. Materials and Methods

In the substrate preparation, the p-type silicon (100) substrate was cut to form a rectangle with a size of 1 cm² then washed using double distilled water [11,12,17–20]. The materials used in the synthesis of BST with different Ba ratio ($x = 0.000; 0.125; 0.250; 0.375; 0.500$) were barium acetate [$\text{Ba}(\text{CH}_3\text{COO})_2$, 99%], strontium acetate [$\text{Sr}(\text{CH}_3\text{COO})_2$, 99%], titanium isopropoxide [$\text{Ti}(\text{C}_{12}\text{O}_4\text{H}_{28})$, 99.999%], The chemicals were calculated and weighed, corresponding to the stoichiometrical composition of $\text{Ba}_x\text{Sr}_{1-x}\text{TiO}_3$. This material is dissolved with acetic acid [CH_3COOH , 100%] and ethylene glycol [$\text{C}_2\text{H}_6\text{O}_2$]. All of the materials are dissolved with a magnetic stirrer at a speed of 240 rpm. Thin-film BST was overgrown above the p-type silicon substrate with a spin coating technique at 8000 rpm for 30 seconds repeated 3 times. Then, BST films were annealed at 850 °C in the furnace model Vulcan™ with an increasing rate of 1.67 °C for 8 hours [14,20–28].

After that, a thin film is prepared to make an MFS layer. 2 holes in the BST part and 2 holes in the silicon substrate part will be made in contact, the remaining part will be covered with aluminum foil. Making contacts aims to install cables that can be used for characterization using LCR. Each cable is attached to each hole using silver paste [26,29,30].

3. Results and Discussion

The characterization was carried out under 3 different conditions, in the darkroom (0 lux), with lights 4000 lux and 8000 lux. Characterization using LCRmeter produces the value of conductance, capacitance, impedance, etc. The value of conductance can be used to calculate the electric conductivity. Electrical conductivity is represented by σ and is defined as the inverse of the resistivity as shown in equations 1, 2, 3 [12,15,28,31–37].

$$\sigma = \frac{1}{\rho} \quad (1)$$

$$\rho = \frac{RA}{l} \quad (2)$$

$$\frac{1}{R} = G \quad (3)$$

The value of conductance can be used to calculate electric conductivity by equation 4.

$$\sigma = \frac{Gl}{A} \quad (4)$$

where G is conductance obtained from the LCR meter.

The electric conductivity of $\text{Ba}_x\text{Sr}_{1-x}\text{TiO}_3$ thin films under LCR characterization is shown in Figure 1.

Figure 1 shows that the electric conductivity tends to increase with increasing frequency. The various mole fraction produces various electric conductivity. Electric conductivity is also greater when it is given the greater intensity of light. This is due to the valence band to conduction band electrical conductivity increase. More electrons are excited into the conduction band due to irradiated light that causes the current to rise [10,20,32].

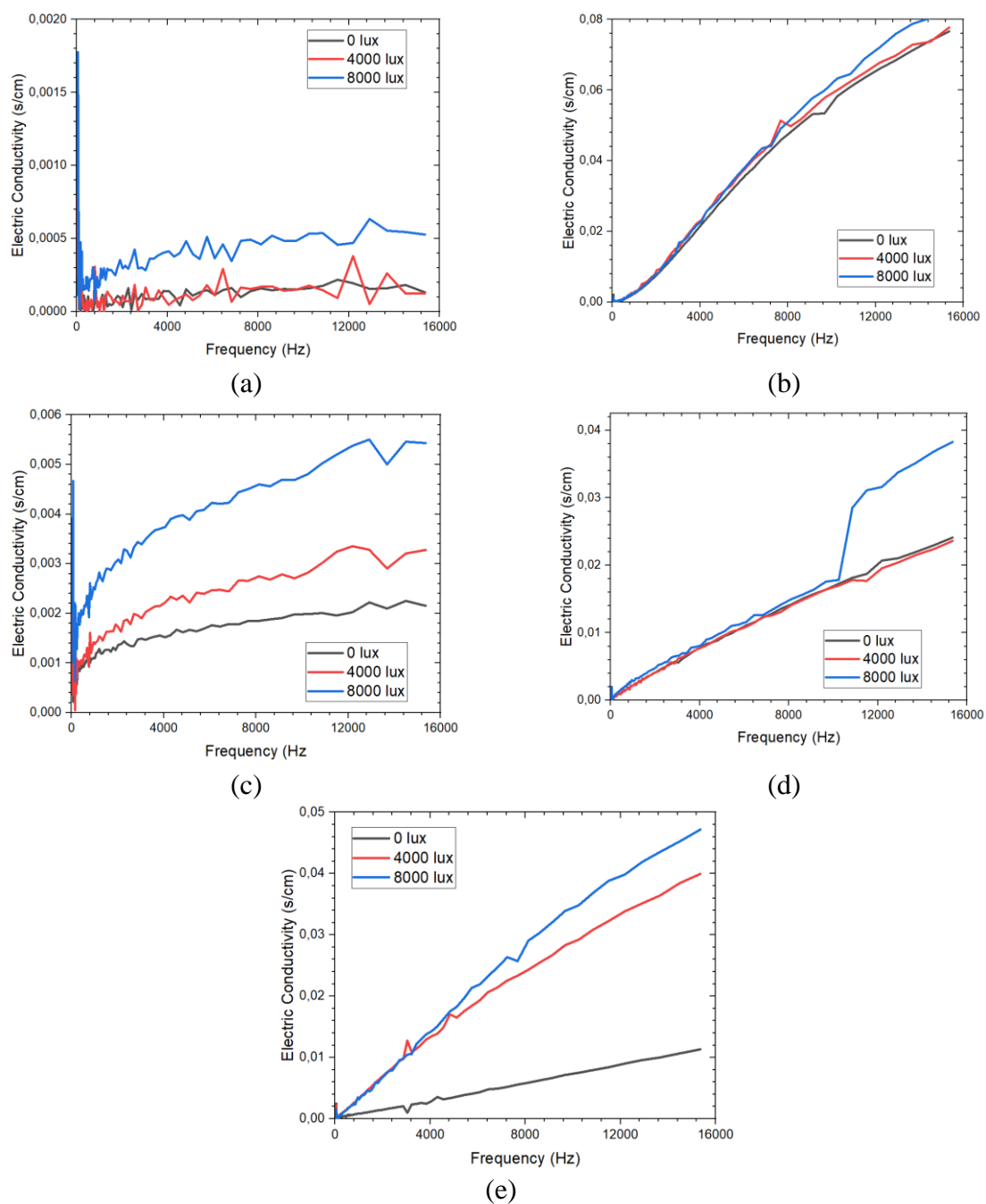


Figure 1/ Electric conductivity as a function of frequency for various mole fraction of BST: **(a)** $x= 0.000$; **(b)** $x= 0.125$; **(c)** $x= 0.250$; **(d)** $x= 0.375$; **(e)** $x= 0.500$.

Thus, the amount of light intensity indicates the energy given to films so that the light intensity will vary directly with electric conductivity.

The capacitance (C) was measured on the LCR meter used to get the dielectric constant (ϵ) that calculated using equation [1,12,37–40]:

$$\epsilon = \frac{Cd}{\epsilon_0 A} \quad (5)$$

where ϵ_0 is the permittivity of free space 8.85×10^{-12} F/m), A is the electrodes' area, and d is the sample's thickness.

The graphs below show the relationship between the dielectric constant and the frequencies that tend to be inversely proportional. Variation of the mole fraction produces different dielectric constant graphs. The dielectric constant's value tends to go up from the mole fraction from 0 to 0.25 and down to the mole fraction from 0.375 to 0.5.

The dielectric constant of $\text{Ba}_x\text{Sr}_{1-x}\text{TiO}_3$ thin films from LCR characterization is shown in Figure 2.

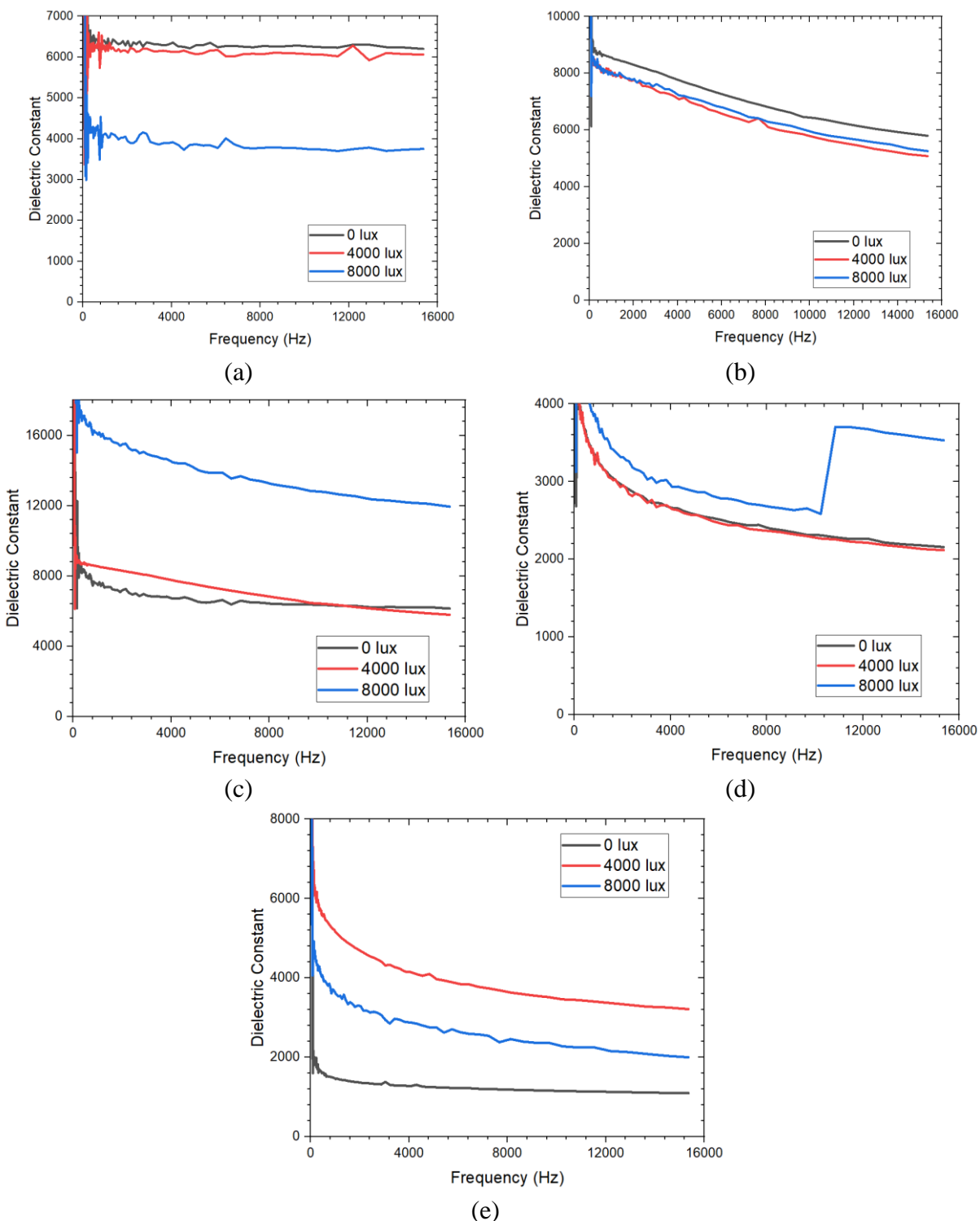


Figure 2. Dielectric constant as a function of frequency for various mole fraction of BST: (a) $x = 0.000$; (b) $x = 0.125$; (c) $x = 0.250$; (d) $x = 0.375$; (e) $x = 0.500$.

The electric conductivity obtained from Eq. 4 can be used to calculate the diffusion coefficient by the equation below [12,32,41]:

$$D = k \frac{KT}{Cq^2} \sigma \quad (6)$$

σ is the electrical conductivity, C and q is the charge of the concentration and imperfections, k depends on the kinds of imperfections; k = 1 for the interstitial ion, k and T are the Boltzmann constant and temperature.

The diffusion coefficient of $\text{Ba}_x\text{Sr}_{1-x}\text{TiO}_3$ thin films from LCR characterization is shown in Figure 3.

Figure 3 shows that the diffusion coefficient tends to increase with increasing frequency. That is because the diffusion coefficient depends on the electric conductivity value, which is directly proportional to the frequency, and that also causes this figure to have the same pattern as Figure 1.

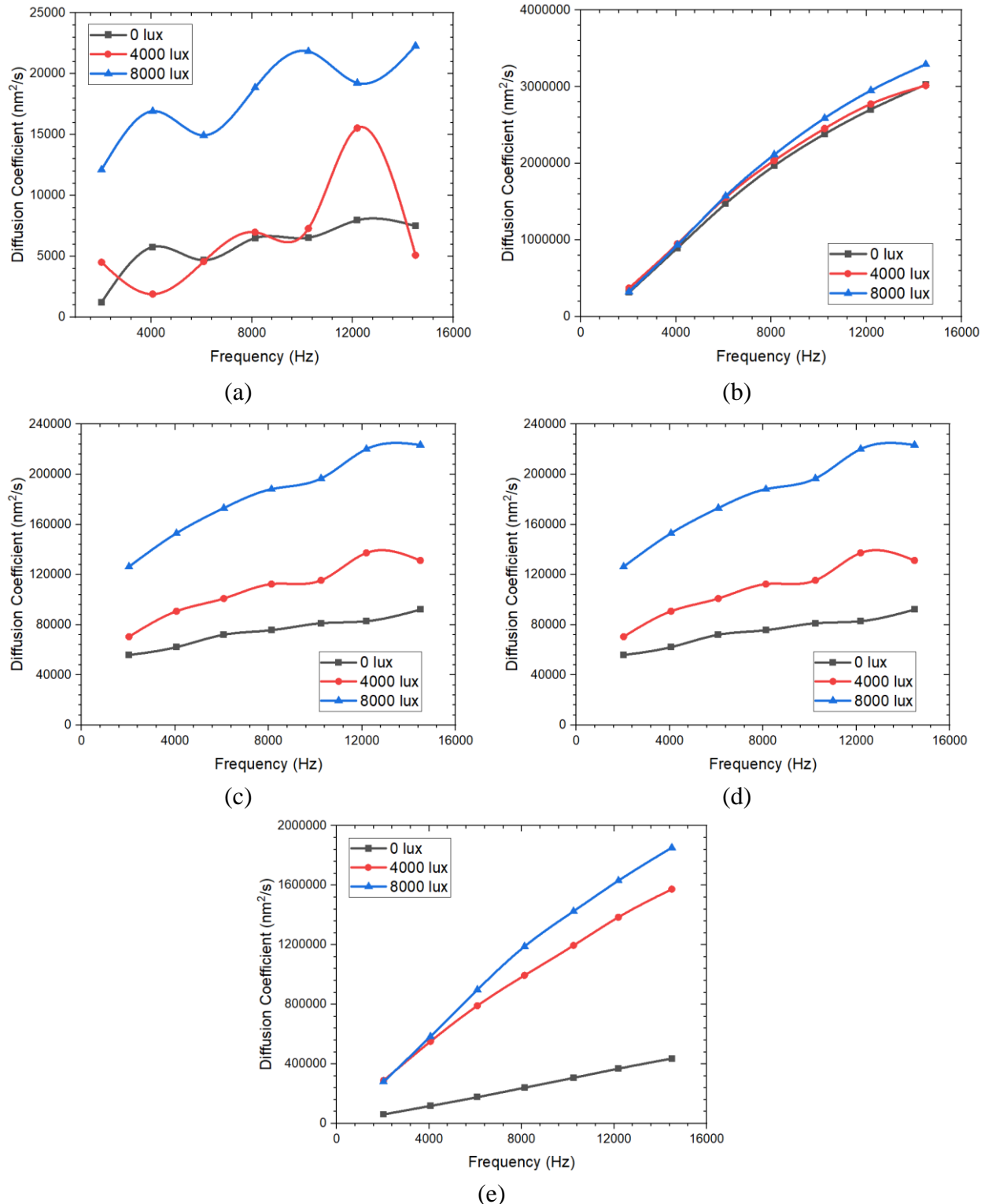


Figure 3. Diffusion coefficient as a function of frequency for various mole fraction of BST: (a) $x = 0.000$; (b) $x = 0.125$; (c) $x = 0.250$; (d) $x = 0.375$; (e) $x = 0.500$.

4. Conclusions

Has succeeded in making thin films based on thin film $BaxSr_{1-x}TiO_3$ ($x = 0.000; 0.125; 0.250; 0.375; 0.500$) with the effect of photoconductive mole fraction and its characterization on electrical properties and diffusivity coefficient.

Funding

This research was funded by Hibah Program Penelitian Kolaborasi Indonesia (PPKI) Kementerian Pendidikan dan Kebudayaan Republik Indonesia, grant number 2011/IT3.L1/PN/2020.

Acknowledgments

The authors declare no acknowledgments.

Conflicts of Interest

The authors declare no conflict of interest. The funders had no role in the study's design, in the collection, analyses, or interpretation of data, in the writing of the manuscript, or in the decision to publish the results.

References

1. Rawat, N.S.; Chawla, M.; Rawat, S.; Fahim, M. Dielectric Behavior of Perovskite Barium Titanate and Barium Strontium Titanate Ceramics. *International Journal of Scientific Research* **2015**, *4*, 3–6, <https://doi.org/10.36106>.
2. Knauss, L.A.; Pond, J.M.; Horwitz, J.S.; Chrisey, D.B.; Mueller, C.H.; Treece, R. The Effect of Annealing on the Structure and Dielectric Properties of $BaxSr_{1-x}TiO_3$ Ferroelectric Thin Films. *Appl. Phys. Lett.* **1996**, *69*, 25–27, <https://doi.org/10.1063/1.118106>.
3. Mulyadi; Wahyuni, R.; Hardhienata, H.; Irzaman Barium strontium titanate thin film growth with variation of lanthanum dopant compatibility as sensor prototype in the satellite technology. *IOP Conf. Ser. Earth Environ. Sci.* **2018**, *149*, <https://doi.org/10.1088/1755-1315/149/1/012069>.
4. Xu, Z.; Yan, D.; Xiao, D.; Yu, P.; Zhu, J. multilayer thin films prepared by RF magnetron sputtering. **2013**, *39*, 1639–1643, <https://doi.org/10.1088/1755-1315/149/1/012069>.
5. Patel, N.D.; Mangrola, M.H.; Soni, K.G.; Joshi, V.G. Structural and Electrical Properties of Nanocrystalline Barium Strontium Titanate. *Mater. Today Proc.* **2017**, *4*, 3842–3851, <https://doi.org/10.1016/j.matpr.2017.02.282>.
6. Teh, Y.C.; Ong, N.R.; Sauli, Z.; Alcain, J.B.; Retnasamy, V. Barium Strontium Titanate (BST) Thin Film Analysis on different layer and annealing temperature. *AIP Conference Proceedings* **2017**, *020290*, <https://doi.org/10.1063/1.5002484>.
7. Szafraniak, B.; Fu, Ł. Semiconducting Metal Oxides: $SrTiO_3$, $BaTiO_3$ and $BaSrTiO_3$ in Gas-Sensing Applications: A Review. *Coating* **2021**, *11*, 1–22, <https://doi.org/10.3390/coatings11020185>.
8. Hamdani, A.; Komaro, M.; Irzaman A synthesis of $BaX Sr_{1-x} TiO_3$ film and characterization of ferroelectric properties and its extension as random access memory. *Mater. Phys. Mech.* **2019**, *42*, 131–140, https://doi.org/10.18720/MPM.4212019_11.
9. Irzaman; Siskandar, R.; Nabilah, N.; Aminullah; Yuliarto, B.; Hamam, K.A.; Alatas, H. Application of lithium tantalate ($LiTaO_3$) films as light sensor to monitor the light status in the Arduino Uno based energy-saving automatic light prototype and passive infrared sensor. *Ferroelectrics* **2018**, *524*, 44–55, <https://doi.org/10.1080/00150193.2018.1432842>.
10. Irzaman, Ridwan Siskandar, . Characterization of $Ba0.55Sr0.45TiO_3$ films as light and temperature sensors and its implementation on automatic drying system model. **2016**, *168*, 130-150, <https://doi.org/10.1080/10584587.2016.1159537>.

11. Irzaman, Ridwan Siskandar, Brian Yuliarto, Mochammad Zakki Fahmi, Ferdiansjah, . Application of Ba 0 . 5 Sr 0 . 5 TiO 3 (Bst) Film Doped with Arduino Nano-Based Bad Breath Sensor. *Chemosensor* **2020**, 8, 3, <https://doi.org/10.3390/chemosensors8010003>.
12. Batalov, R.I.; Zharkov, D.K.; Pavlov, D.P.; Migachev, S.A.; Lunev, I. V.; Elshin, A.S.; Leontyev, A. V.; Chibirev, A.O.; Shaposhnikova, T.S.; Mamin, R.F. Properties of the barium strontium titanate film on the silicon substrate. *Ferroelectrics* **2020**, 559, 30–35, <https://doi.org/10.1080/00150193.2020.1722003>.
13. Nur Aidi, M.; Irzaman Best stochastics model for percentage of transmittance of lithium niobate affected by wavelength of visible light. *Ferroelectrics* **2020**, 558, 222–239, <https://doi.org/10.1080/00150193.2020.1735906>.
14. Zaoui, M.; Sellami, B.; Boufahja, F.; Faloda, F.; Nahdi, S.; Alrezaki, A.; Alwasel, S.; Harrath, A.H. Effects of ferroelectric oxides of barium strontium titanate (Ba0.85Sr0.15TiO3) nanoparticles on Ruditapes decussatus assessed through chemical, physiological, and biochemical methods. *Chemosphere* **2021**, 265, 129078, <https://doi.org/10.1016/j.chemosphere.2020.129078>.
15. Djohan, N.; Harsono, B.; Liman, J.; Hardhienata, H.; Husein, I. The effect of indium oxide (In2O3) dopant on the electrical properties of LiTaO3 thin film-based sensor. *Ferroelectrics* **2020**, 568, 55–61, <https://doi.org/10.1080/00150193.2020.1811031>.
16. Anindy, U.; Nur Indro, M.; Husein, I. Piezoelectric properties: cerium oxide (CeO2) doped barium titanate (BaTiO3) film on ITO substrate. *Ferroelectrics* **2021**, 570, 162–175, <https://doi.org/10.1080/00150193.2020.1839267>.
17. Palupi, E.K.; Umam, R.; Andriana, B.B.; Sato, H.; Yuliarto, B.; Alatas, H.; Irzaman Micro-Raman analysis of Ba0.2Sr0.8TiO3 (barium strontium titanate) doped of chlorophyll of cassava leaf. *Ferroelectrics* **2019**, 540, 227–237, <https://doi.org/10.1080/00150193.2019.1611116>.
18. Irzaman; Nuraisah, A.; Aminullah; Hamam, K.A.; Alatas, H. Optical properties and crystal structure of lithium doped Ba 0.55 Sr 0.45 TiO 3 (BLST) thin films. *Ferroelectr. Lett. Sect.* **2018**, 45, 14–21, <https://doi.org/10.1080/07315171.2018.1499361>.
19. Setiawan, A.; Palupi, E.K.; Umam, R.; Alatas, H.; Irzaman Optical characterization of Ba0.5Sr0.5TiO3 material grown on a p-type silicon substrate (111) doped niobium oxide and chlorophyll. *Ferroelectrics* **2020**, 568, 62–70, <https://doi.org/10.1080/00150193.2020.1735893>.
20. Kurniawan, A.; Irzaman; Yuliarto, B.; Fahmi, M.Z.; Ferdiansjah Application of barium strontium titanate (BST) as a light sensor on led lights. *Ferroelectrics* **2020**, 554, 160–171, <https://doi.org/10.1080/00150193.2019.1684758>.
21. Rahmawaty, V.; Sumaryada, T.; Irzaman Optical properties and microstructure rietveld analysis of CeO2-doped SrTiO3 thin film. *AIP Conf. Proc.* **2019**, 2202, <https://doi.org/10.1063/1.5141722>.
22. Pamungkas, N.G.; Dahrul, M.; Irzaman; Alatas, H. Optical properties of Cu and Ru doped BST thin films with additive glycerol and MESA surfactant. *IOP Conf. Ser. Earth Environ. Sci.* **2017**, 65, 0–7, <https://doi.org/10.1088/1755-1315/65/1/012031>.
23. Irzaman; Zuhri, M.; Novitri; Irmansyah; Setiawan, A.A.; Alatas, H. Surface Morphology Properties Doped RuO2 (0, 2, 4, 6%) of Thin Film LiNbO3. *J. Phys. Conf. Ser.* **2019**, 1282, 0–6, <https://doi.org/10.1088/1742-6596/1282/1/012040>.
24. Arshad, M.; Du, H.; Javed, M.S.; Maqsood, A.; Ashraf, I.; Hussain, S.; Ma, W.; Ran, H. Fabrication, structure, and frequency-dependent electrical and dielectric properties of Sr-doped BaTiO3 ceramics. *Ceram. Int.* **2020**, 46, 2238–2246, <https://doi.org/10.1016/j.ceramint.2019.09.208>.
25. Mohit; Murakami, T.; Haga, K.I.; Tokumitsu, E. Impact of annealing environment on electrical properties of yttrium-doped hafnium zirconium dioxide thin films prepared by the solution process. *Jpn. J. Appl. Phys.* **2020**, 59, <https://doi.org/10.35848/1347-4065/aba50b>.
26. Rahmawaty, V.; Palupi, E.K.; Patonah, N.; Sumaryada, T.; Irzaman. The Mole Fraction Effect on Magnetic Properties of BaxSr1-xTiO3 (x = 0; 0.125; 0.25; 0.375; 0.500) Thin Film. *Key Eng. Mater.* **2020**, 855, 197–201, <https://doi.org/10.4028/www.scientific.net/KEM.855.197>.
27. Rini, R.P.; Nurosyid, F.; Iriani, Y. The effects of annealing temperature and angular velocity variation on microstructure and optical properties of barium titanate (BaTiO3) using chemical solution deposition method. *J. Phys. Conf. Ser.* **2019**, 1397, <https://doi.org/10.1088/1742-6596/1397/1/012001>.
28. Mohammed, B.; Kaleli, M. Effect of Substrate and Annealing Ambient on the Conductivity of Sputtered MoSi2 Ceramic Thin Film. *J. Electron. Mater.* **2020**, 49, 5570–5584, <https://doi.org/10.1007/s11664-020-08282-9>.

29. Irzaman; Syafutra, H.; Rancasa, E.; Nuayi, A.W.; Rahman, T.G.N.; Nuzulia, N.A.; Supu, I.; Sugianto; Tumimomor, F.; Suriandy; et al. The effect of Ba/Sr ratio on electrical and optical properties of Ba x Sr (1-x)TiO₃ (x = 0.25; 0.35; 0.45; 0.55) thin film semiconductor. *Ferroelectrics* **2013**, *445*, 4–17, <https://doi.org/10.1080/00150193.2012.742351>.
30. Misbakhushudur, M.; Ismangil, A.; Aminullah; Irmansyah; Irzaman Phasor Diagrams of Thin Film of LiTaO₃ as Applied Infrared Sensors on Satellite of LAPAN-IPB. *Procedia Environ. Sci.* **2016**, *33*, 615–619, <https://doi.org/10.1080/00150193.2012.742351>.
31. Heaney, M.B. Electrical Conductivity and Resistivity. **2003**.
32. Ismangil, A; Irmansyah; Irzaman. The diffusion coefficient of lithium tantalite (LiTaO₃) with temperature variations on LAPAN-IPB satellite infra-red sensor. *Procedia Environmental Sciences* **2016**, *33*, 668–673, <https://doi.org/10.1016/j.proenv.2016.03.122>.
33. Irzaman; Putra, I.R.; Aminullah; Syafutra, H.; Alatas, H. Development of Ferroelectric Solar Cells of Barium Strontium Titanate (Ba_xSr_{1-x}TiO₃) for Substituting Conventional Battery in LAPAN-IPB Satellite (LISAT). *Procedia Environ. Sci.* **2016**, *33*, 607–614, <https://doi.org/10.1016/j.proenv.2016.03.114>.
34. Auromun, K.; Choudhary, R.N.P. Structural, Dielectric and Electrical investigation of Zirconium and Tin modified 0.5BFO-0.5BST. *Mater. Chem. Phys.* **2020**, *250*, 123033, <https://doi.org/10.1016/j.matchemphys.2020.123033>.
35. Gudkov, S.I.; Solnyshkin, A. V.; Kiselev, D.A.; Belov, A.N. Electrical conductivity of lithium tantalate thin film. *Ceramica* **2020**, *66*, 291–296, <https://doi.org/10.1590/0366-69132020663792885>.
36. Ismangil, A.; Prakoso, W.G. The Effect of Electrical Conductivity of LiTaO₃ Thin film to Temperature Variations. *International Journal of Advanced Science and Technology* **2020**, *29*, 3234–3240.
37. Iriani, Y.; Nurosyid, F.; Setyadi, A.U.L.S. The effect of mole concentrations of Sr-doped of BAI. X Sr x TiO₃ film on microstructure, optical, and electrical properties. *AIP Conf. Proc.* **2020**, *2296*, <https://doi.org/10.1063/5.0032543>.
38. Raimarda, R.; Zulfa, I.L.; Irzaman, I. Formulation of 2nd rank tensor algorithm to calculate quadrupole moment and electric potential of Plumbum Zirconium Titanate (PZT) material. *AIP Conf. Proc.* **2019**, *2169*, <https://doi.org/10.1063/1.5132690>.
39. Dewi, R. Optical characterization of Ba 1-X Sr x TiO₃ thin film properties using ultraviolet-visible spectroscopy. *AIP Conf. Proc.* **2020**, *040001*, <https://doi.org/10.1063/5.0003054>.
40. Bintari, P.L.; Rahmawaty, V.; Palupi, E.K.; Patonah, N.; Irmansyah; Sumaryada, T.; Irzaman Effect of light intensity on magnetic properties of srtio3 thin-films. *Key Eng. Mater.* **2020**, *855 KEM*, 208–212, <https://doi.org/10.4028/www.scientific.net/KEM.855.208>.
41. Zaghet, M.A.; Varela, J.A.; Gonza, A.H.M. Effect of preannealing on the morphology of LiTaO₃ thin films prepared from the polymeric precursor method. *Materials Characterization* **2003**, *50*, 233–238, [https://doi.org/10.1016/S1044-5803\(03\)00098-6](https://doi.org/10.1016/S1044-5803(03)00098-6).